

Effect of Process Parameters on the Electrodeposition of Zinc on 1010 Steel: Central Composite Design Optimization

Mehmet Kul¹, Kürşad Oğuz Oskay², Fuat Erden^{1,*}, Erdem Akça², Ramazan Katırcı³, Erkan Köksal², Evindar Akıncı²

¹ Sivas University of Science and Technology, Department of Aeronautical Engineering, 58050, Sivas, Turkey

² Cumhuriyet University, Department of Metallurgical and Materials Engineering, 58140, Sivas, Turkey

³ Sivas University of Science and Technology, Department of Metallurgical and Materials Engineering, 58050, Sivas, Turkey

*E-mail: fuaterden@sivas.edu.tr

Received: 7 May 2020 / Accepted: 17 July 2020 / Published: 31 August 2020

In the present work, we studied the effect of critical electrogalvanizing parameters on the quality of electrodeposited Zn films. The current density, electrodeposition time, and ZnCl₂ concentration of electrolyte were optimized to maximize current efficiency and brightness, and also, to minimize the surface roughness. Importantly, regression models of the response variables were developed. These models could help industrial applications by providing definitive process conditions to obtain Zn coatings at a desired thickness, roughness and brightness with a high current efficiency. First, preliminary studies were conducted to determine the initial levels of the designated factors. Then, the optimization was conducted through the Central Composite Design by Design-Expert (trial version). Upon completion of the optimization, analysis of variance was also performed. The optimum values of current density, coating duration and ZnCl₂ concentration were determined as 3.7 A/dm², 4.4 minutes, and 50 g/L, respectively, at a thickness of 6 μm. Finally, a set of Zn films were deposited at this optimum conditions. The characterization of these films showed that the experimental results were in good accordance with model predictions, providing a bright (L*=83.69) and smooth (Ra=0.75 μm) coating with excellent adhesion to steel substrate (pull-off strength > 29.4 MPa) at a current efficiency of 98.7%.

Keywords: Electrogalvanizing, Central composite design, Zinc coating, Electrodeposition

1. INTRODUCTION

Steel is the most widely used material in various industrial applications thanks to its outstanding mechanical properties. On the other hand, steel's main drawback is its low resistance to corrosion, which is often addressed by coating its surface with a protective layer. Zinc (Zn) has received considerable

attention as a protective coating material, since it could provide improved corrosion protection even in relatively aggressive environments [1, 2]. Zinc coating, due to its low standard electrode potential ($E^{\circ} = -0.76$ V vs SHE), acts as a sacrificial coating on steel [2]. Such coating on the metal surface is generally prepared by hot dip galvanizing, electrogalvanizing, ion vapour deposition and metal spray coating methods [3-10]. Among them, hot dip galvanizing suffers from the necessity of high temperatures, vapour deposition is expensive and high porosity is the main drawback of spray coating [3, 4, 9, 10]. Accordingly, electrolytic coating of Zn becomes the most frequently employed technique in the field.

Regarding electrodeposition of Zn, it has been extensively carried out in acidic and alkaline baths [11-13]. Among them, acidic baths are commonly preferred since the efficiency of acidic electrodeposition baths is higher and their maintenance is easier than that of alkaline baths [14]. In the acidic electrodeposition bath of Zn, various types of inorganic and organic chemicals are used to enhance the surface morphology of deposits (grain size, brightness, porosity etc.) and the crystal structure of zinc grains [1, 2, 15-22]. These additives could also improve the current yield, thickness distribution and cathodic polarization [1, 2, 15-17, 20]. The most commonly used traditional additives include glue, gelatin and gum, however, they have high toxicity and low thermal stability [15]. Alternatively, Trejo et al. introduced polyethylene glycol (PEG) as an additive during the electrodeposition of Zn in an acidic bath and reported that the morphology of deposits shifted towards a nodular structure, together with increasing grain size in the presence of PEG [20]. Besides, they noted that the presence of PEG also altered the corrosion rate, depending on the molecular weight (MW), while PEG with 8000 MW provided the lowest corrosion rate in their study [20]. Recently, Rocca et al. investigated the influence of nettle extract (NE) on the Zn electrodeposition and found that NE, as an additive, lowered the cathodic current density and reduced the proton adsorption onto steel, and thus leading a larger cathodic overpotential of hydrogen evolution, as well as providing finer grains [1].

In fact, most of the previous studies focused on the introduction of such additives in Zn electrodeposition. However, a detailed investigation regarding the effect of process parameters, but the additives, on the yield and quality of the deposited Zn film is also crucial. This is because the current efficiency and surface roughness, together with the associated texture and brightness, are well-known to affect the corrosion behavior of final coating [23-26]. Thus, the optimization of process parameters to maximize current efficiency and surface finish by statistical design of experiments software will particularly be of great importance. Use of central composite design (CCD) is an efficient way for such optimization studies, and there are several reports in which the electrodeposition of Cu-Zn and Zn-Ni alloys were investigated through CCD [27-30]. On the other hand, we studied the electrodeposition of Zn metal in the present work, with a particular focus on the statistical optimization of process parameters such as the amount of Zn in the electrolyte, current density and duration of electrodeposition. The effects of these parameters on the current efficiency, roughness and brightness of the electrodeposited Zn films were investigated. The CCD was used through Design-Expert software (trial version) and the statistically evaluated data were compared with experimental results to optimize the afore-mentioned process parameters. Importantly, regression models, which could be used in industrial applications for the anticipation of process parameters to provide desirable Zn coatings, were developed. The analysis of variance (ANOVA) was also conducted to confirm the validity of CCD. Upon optimization of the current

density, ZnCl_2 concentration and electrodeposition time, the optimized Zn coating was also characterized in detail, showing excellent adhesion to the steel substrate.

2. EXPERIMENTAL

2.1. Methods and materials

SAE 1010 steel substrates with dimensions 20x100x1 mm were used as cathode. A pre-treatment process was applied on these substrates first to remove the unwanted contaminants such as oil, rust and dirt from their surfaces. In the first step of pretreatment, the samples were dipped in 50 vol% H_2SO_4 etching solution for 5 min and rinsed with distilled water. Later, the specimens were grinded with sandpaper and subsequently cleaned in a soap solution. The samples were degreased in 10 wt% HCl solution for 1 minute at 60-80 °C and then rinsed with distilled water. Finally, the samples were electrocleaned at a current density of 2.5 A/dm^2 for 1 min.

Following this, Zn coatings were prepared on the pretreated 1010 steel substrates under galvanostatic conditions at room temperature for various durations, using a direct current generator (model MCH-305B 30V 5A). During the tests, Zn plates, whose dimensions are the same as the 1010 steel cathode, were used as anode. The electroplating bath is made of mica and the dimensions of the cell are 5x5x12 cm. The volume of the bath is 275 mL and the bath was agitated with a magnetic stirrer at 100 rpm. The distance between the anode and cathode was maintained constant. The experimental setup is shown in Figure 1.



Figure 1. The experimental setup in which Zn coating was performed

An acidic bath containing Zn was prepared with the following composition: 40 g/L zinc chloride, 120 g/L ammonium chloride, 0.02 mL/L brightener and 0.2 mL/L make up solution. This bath was named as Zn-A bath. The concentration of ammonium chloride, brightener and make up solution were maintained constant during the experimental studies. The ZnCl₂ concentration of the bath, as well as the current density and coating duration were specified as the factors to optimize the Zn coating. The central composite experimental design (CCD) was used to optimize these parameters by Design-Expert software (trial version). The initial levels of these factors were determined based on our preliminary studies. Then, the experimental results were compared with the model predictions of Design-Expert (trial version), and the analysis of variance (ANOVA) was conducted to check the validity of CCD.

2.2. Characterization

The current efficiency was calculated by dividing the measured weight of the deposited Zn to its theoretical weight and then multiplying by 100. The 1010 steel cathode substrates were weighted both prior to and following electrodeposition tests, and the actual weights of Zn films were determined by the difference. The theoretical amount of Zn metal coated at the cathode was calculated from the following equation:

$$W = Mit/nF \quad \text{Eq. 1}$$

In equation 1, W shows the theoretical weight of the metal deposited at the cathode in grams, M represents the atomic mass of the metal, I is the current, t is the processing time in seconds, n is the molar number of electrons consumed in the reduction reaction and F is the Faraday constant (~96500 C/mole).

The adhesion test was conducted to determine the pull-off strength and to comment on the quality of deposited films. The Zn films on steel substrates and the surfaces of 10mm diameter Al dollies were first roughened to enhance bonding of the adhesive, and washed by ethanol and DI water, and then finally dried overnight. Following this, epoxy based adhesive was prepared and applied to the Zn films through the Al dollies. The excess epoxy was removed via acetone and the Al dollies on Zn films were kept at room temperature for 24 hours for curing. Following this, the adhesion tests were finally carried out by PosiTect At-M.

Tescan Mira3 scanning electron microscope (SEM) was used for microstructural imaging and EDX analysis. The surface roughness was recorded using a TMR200 surface roughness gauge. Mitutoyo micrometer was used to measure the thickness of the coatings.

Color measurements were conducted using Konica Minolta CM-700d Spectrophotometer based on the CIE L*a*b colour space as defined by the International Commission on Illumination (CIE). Here, L* refers to the lightness value and covers the range of darkest black at L*=0 to brightest white at L*=100, and thus the L* was used in the present work as the indicator of brightness. The a* axis and b* axis represent green/red and blue/yellow coordinates, respectively. Following a calibration with a perfect white (L*: 100, a*=b*=0) reference, the measurements were conducted under C illuminant at a 2 degree standard observer. Yellowness Index (YI) was calculated as well according to ASTM D1925 standard.

3. RESULTS AND DISCUSSION

3.1. Determination of optimization levels

The factors to be optimized in electrodeposition of Zn regarding coating quality were chosen as current density, coating duration and the concentration of ZnCl_2 in deposition bath. First, preliminary studies were conducted to determine the initial levels of these factors for CCD.

A series of experiments were performed to investigate the effect of current density on current efficiency, and to determine the minimum and maximum values of current density for optimization studies. Zn-A bath was used for these experiments. The duration and temperature were specified as 5 minutes and room temperature, respectively, and both kept constant during the tests. The current density was changed in the range of 0.8-16.8 A/dm^2 . The surface area of the steel cathodes was 0.125 dm^2 .

The current efficiency was evaluated as explained in section 2.2 and plotted against current density. As can be seen from Figure 2(a), the current efficiency increased with the current density up to $\sim 5 \text{ A}/\text{dm}^2$. Then, exceeding this current density resulted in the loss of current efficiency. This was ascribed to the hydrogen evolution reaction, and is in good accordance with the previous reports [31-37]. As a result of over-increasing the current density, more part of the current might be used for hydrogen evolution, causing a decrease in the amount of deposited Zn, and hence, reducing the current efficiency [32-38].

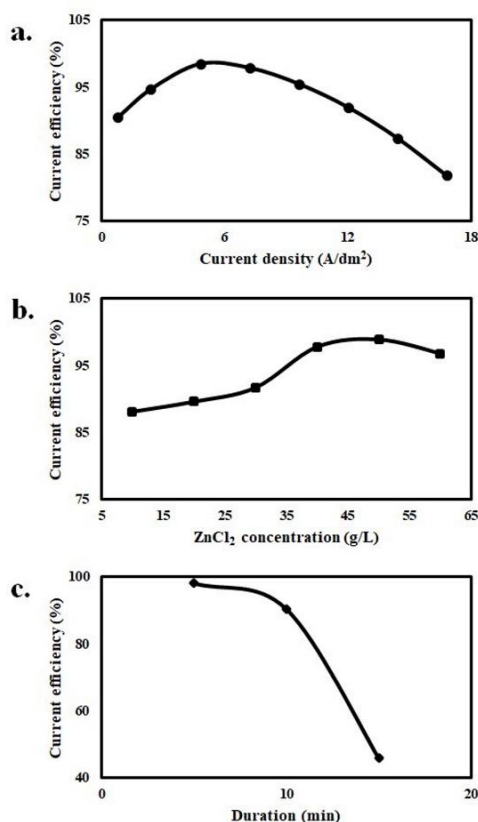


Figure 2. Effect of current density (a), ZnCl_2 concentration (b), and electrodeposition time (c) on the current efficiency of Zn electrodeposition

In fact, hydrogen evolution is a serious issue in Zn electrodeposition since the evolved hydrogen could be adsorbed at the surface [35, 39]. One hypothesis was that hydrogen might be absorbed by the steel before the first Zn crystallizes since the overpotential of hydrogen evolution is lower on steel [35, 39]. However, Casanova et al showed that this is not valid due to the strong underpotential deposition of Zn [39]. Second mechanism is the trapping of hydrogen in the Zn film, and its further diffusion to the substrate [35, 36, 39-42]. Previous studies showed that hydrogen is first adsorbed, but its major part could be released as a gas via Tafel recombination depending on the deposition parameters and surface quality [31, 35, 36, 40-42]. Yet, a fraction of the absorbed hydrogen could still diffuse to the steel, deteriorate its mechanical properties and might cause hydrogen embrittlement [34, 35, 39-41]. One way to reduce hydrogen permeation is to reduce the current density, and higher current efficiency might also be an indicator of less hydrogen absorption to the steel [31, 35].

Moreover, Eq. 1 shows that the amount of metal deposited per unit time is increasing with current. However, upon increasing the current density above a critical limit, burning of the deposits and/or additives might occur, deteriorating the quality of the coating [38, 43-45]. These kinds of coatings are termed as burnt deposits. Indeed, the optical microscope images, as given in Figure 3(a and b), showed that the deposit was burnt in appearance when the current density increased. This was possibly another factor causing the loss of current efficiency at relatively higher current densities.

Overall, the minimum and maximum levels of the current density to initiate the optimization procedure were determined as 2 A/dm², and 7 A/dm², respectively. This is because the current efficiencies were too low outside this region, might indicate a hydrogen absorption problem, and also resulted in rough and dark films, especially at high current densities.

Another set of experiments were carried out to investigate the effect of ZnCl₂ concentration in electrolyte, and to determine the minimum and maximum values of ZnCl₂ concentration for optimization studies. In these tests, the zinc chloride concentration varied from 10 g/L to 60 g/L, while keeping other components of the Zn-A bath constant. The current density was set to 5.2 A/dm², the temperature was room temperature and the duration was 5 min. Figure 2(b) shows that increasing the zinc chloride concentration resulted in the enhancement of current efficiency up to 50 g/L, which is in good accordance with the previous reports [27, 46]. The presence of more metal ions in electrolyte increased the carrier concentration, and hence the ionic conductivity. Besides, the diffusion rate at the electrode/electrolyte interlayer would be possibly faster due to a larger driving force upon increasing the Zn²⁺ concentration of electrolyte, also boosting the current efficiency. Moreover, Mirkova et al. reported that the hydrogen absorption into steel not only depends on current density, but also on the ZnCl₂ concentration [35]. Excessive hydrogenation might occur on the substrate at low ZnCl₂ concentrations due possibly to the porous nature of the film [35, 47]. However, the hydrogen permeation rate was reported to decrease with increasing ZnCl₂ concentration as a result of the higher compactness of denser coatings [35, 47]. On the other hand, the enhancement in current efficiency tended to stop at 50 g/L, which was ascribed to the increasing viscosity and decreasing carrier mobility as a result of introducing excessive metal ions to the electrolyte. Accordingly, the minimum and maximum levels of the ZnCl₂ concentration for optimization studies were determined as 10 g/L and 50 g/L, respectively.

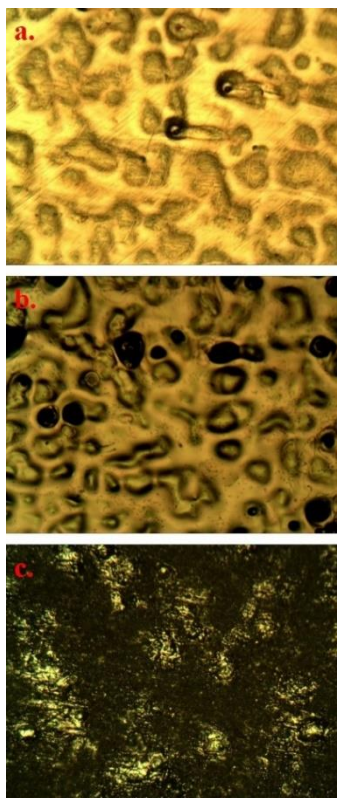


Figure 3. Optical microscope images of the Zn coatings deposited in Zn-A bath at the current density of 2.4 A/dm² for 5 min (a), 16.8 A/dm² for 5 min (b) and 5.2 A/dm² for 15 min (c)

In another set of experiments, the electrodeposition time was varied between 5, 10 and 15 minutes, while keeping ZnCl₂ concentration and current density constant at 40 g/L and 5.2 A/dm², respectively. As can be seen from Figure 2(c), the current efficiency decreased with increasing electrodeposition time, especially when it was increased to 15 minutes. Most of the Zn ions might already be used to form a layer at the cathode electrode-electrolyte interface long before 15 minutes, and the rate greatly reduced afterwards as the $\text{Zn}^{2+} + 2\text{e} = \text{Zn}$ reaction cannot take place any longer. In other words, there were no sufficient ions existing anymore at the cathode when the duration reached 15 minutes. In this case, most of the current was likely to be consumed for the side reactions such as $2\text{H}^+ + 2\text{e} = \text{H}_2(\text{g})$, giving rough, porous, burnt and brittle coatings. Besides, the hydrogen evolution might also cause the pH to increase and the solution became basic, causing zinc coating to redissolve. This was supported by optical microscope images in Figure 3(c), which shows that the surface was heavily burnt when the coating duration was 15 minutes. Since the efficiency decreased when the electrodeposition was longer than 5 min, the minimum and maximum levels of the electrodeposition time for the optimization studies were determined as 2 and 5 min, respectively.

3.2. Optimization studies

The initial levels of the current density, coating duration and ZnCl₂ concentration were determined based on the preliminary studies as explained in section 3.1 and CCD was applied for the optimization procedure. Factors and levels that used in the CCD were listed in Table 1.

Table 1. Factors and their levels in optimization procedure with CCD

Factors	-1	0	+1
(A) Current density (A/dm ²)	2.0	4.5	7.0
(B) Duration of coating (min)	2	3.5	5
(C) ZnCl ₂ concentration (g/L)	10	30	50

The CCD provided 18 experimental conditions to run the optimization. Electrodeposition tests were conducted under these conditions and the results were inputted to Design-Expert (trial version). Then, the simulation results of Design-Expert (trial version) were compared with actual experimental results in Table 2. Overall, Table 2 shows that the experimental results are in good accordance with the model predictions.

Table 2. The experimental and model prediction results of Zn electrodeposition (A: current density (A/dm²), B: electrodeposition time (min), and C: ZnCl₂ concentration)

No	A	B	C	Experimental Results			Model Results		
				Current Efficiency (%)	Roughness (μm)	Brightness (L)	Current Efficiency (%)	Roughness (μm)	Brightness (L)
1	2	2	50	99.42	0.95	77.95	100.06	0.99	77.73
2	4.5	2	30	95.00	0.46	78.56	92.72	0.96	76.80
3	4.5	3.5	30	91.36	1.3	76.71	91.46	1.12	76.79
4	2	5	10	90.20	1.36	74.88	89.37	1.37	75.45
5	7	5	50	97.23	0.68	80.44	96.93	0.65	80.29
6	7	2	50	98.39	0.82	78.68	99.00	0.76	78.13
7	4.5	5	30	90.78	1.21	80.16	90.21	1.28	76.78
8	2	3.5	30	90.78	1.46	73.23	90.20	1.13	72.52
9	2	5	50	94.30	0.77	79.41	94.99	1.01	79.60
10	2	2	10	92.24	0.63	77.49	92.32	0.62	77.65

11	4.5	3.5	10	88.51	0.75	82.97	91.03	1.12	82.18
12	4.5	3.5	30	91.63	1.28	75.32	91.46	1.12	76.79
13	7	5	10	87.86	1.64	81.37	86.99	1.55	81.60
14	4.5	3.5	30	91.89	1.31	73.73	91.46	1.12	76.79
15	4.5	3.5	30	89.00	1.25	76.17	91.46	1.12	76.79
16	7	3.5	30	87.02	0.7	75.16	88.48	1.11	75.80
17	4.5	3.5	50	101.52	1.04	80.84	99.87	0.85	81.56
18	7	2	10	87.86	1.22	83.69	86.94	0.94	83.52

The model equations for the response variables were developed upon completion of the necessary experiments. These models could be used in industrial applications to determine the process conditions, yielding a desired surface roughness and brightness for the application under consideration. Corresponding equations are presented below, where (A), (B) and (C) represents the current density (A/dm^2), electrodeposition time, and $ZnCl_2$ concentration, respectively:

$$\text{Current efficiency (\%)} = +95.60447 + 1.37007A - 1.20738B - 0.41248C + 0.20021AB + 0.021565AC - 0.017681BC - 0.34018A^2 + 0.00997223C^2$$

$$\text{Surface roughness, Ra (\mu m)} = -0.22062 + 0.10885A + 0.32958B + 0.0255C - 0.009AB - 0.002725AC - 0.006125BC$$

$$\text{Brightness (L)} = +77.45080 + 5.18542A - 1.11458B - 0.77411C + 0.019667AB - 0.027325AC + 0.033958BC - 0.41992A^2 + 0.012714C^2$$

The analysis of variance (ANOVA) was carried out to check the validity of the models. The results of variance analysis were given in Table 3 and Table 4. The statistical significance of variables in the ANOVA table is estimated by their p-values. If the p-value of any variable is lower than 0.05 ($\alpha=0.05$, or 95% confidence), it could be considered as statistically significant. This means that the corresponding variable strongly depends on the optimization factors. In addition to the p-values, F-value could also be used to compare statistical models that have been fitted to a data set. On the other hand, unlike p-values, large F-value is much desirable as it could suggest greater dispersion. Table 3 shows that the current efficiency and coating brightness are statistically significant, because the p-values of quality variables are lower than 0.05 with relatively high F-values. Yet, having a p-value of >0.05 , roughness model could be regarded as statistically insignificant. Overall, the current efficiency has the highest F and lowest P values, suggesting that it is the most affected quality variable by the factors.

Table 3. ANOVA results of the developed models

Variables	R ²	F-values	P- values
Current efficiency (%)	0.913	11.8	0.0006
Roughness (Ra)	0.578	2.5	0.0883
Brightness (gloss)	0.817	5.0	0.0131

Another comparison method is R² values. When this value is close to 1, the data compatibility between the mathematical model and its response is very high. As can be seen in Table 3, the model used for response variables have a percentage R² values close to 1 except the roughness. This denotes that the simulation and experimental results have high compatibility and the model equations of current efficiency and brightness can be used with high confidence to predict actual results.

Table 4. Statistical significance of individual factors and their mutual interactions (A: current density (A/dm²), B: electrodeposition time (min), and C: ZnCl₂ concentration)

Factors	p-values for current efficiency	p-values for roughness	p-values for brightness
A	0.1511	0.8922	0.0185
B	0.0477	0.0718	0.9850
C	< 0.0001	0.0630	0.6027
AB	0.2514	0.7107	0.9106
AC	0.1122	0.1526	0.0610
BC	0.4090	0.0625	0.1450

The p-values in Table 4 suggests that the ZnCl₂ concentration is the most significant factor affecting the current efficiency. Also, as can be seen from Table 4, none of the individual factors are statistically significant for the roughness of the coatings. Regarding brightness, current density is the main factor influencing it. When the mutual interactions among the factors are examined, it could be noticed that AB and BC interactions have no significant effect as compared to AC interaction.

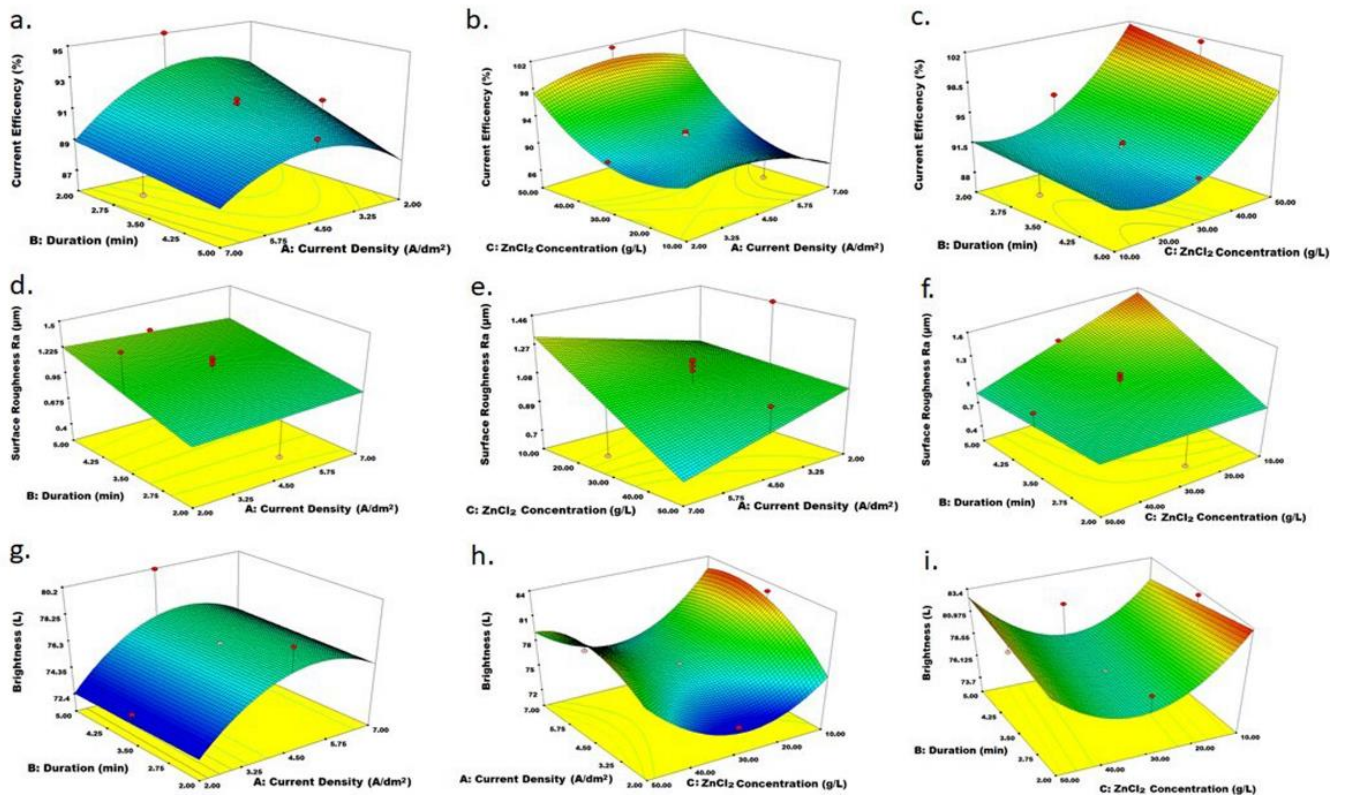


Figure 4. Response surface graphs, illustrating the effect of electrodeposition time – current density (a, d, g), current density – ZnCl₂ concentration (b, e, h) and electrodeposition time – ZnCl₂ concentration (c, f, i) mutual interactions on the current efficiency (a-c), roughness (d-f) and brightness (g-i) of the electrodeposited films.

Figure 4 represents the response surface graphs, further illustrating the effect of individual factors and their mutual interactions on the process variables. When the effects of current density and duration on the current efficiency examined together at a constant ZnCl₂ concentration of 30 g/L in Figure 4(a), it is observed that the current density has an optimum value of about ~4 A/dm². However, considering the effects of ZnCl₂ concentration and current density together at a constant duration of 3.5 min, it can be seen that the current efficiency tends to drop instead when the current density values exceed ~3.5 A/dm². Also, the current density that maximizing efficiency slightly varied depending on the ZnCl₂ concentration as can be seen in Figure 2(b). This could be expected as previous studies already indicated that the rate of hydrogen evolution depends on both current density and electrolyte concentration [35]. Likewise, we found that efficiency is decreasing in both cases, after certain current density values due possibly to the hydrogen evolution reaction. As a result of increasing hydrogen evolution, less Zn²⁺ ions were supplied to the diffusion layer at cathode/electrolyte interface than expected. Regarding concentration, the current efficiency increases with the amount of ZnCl₂ no matter what the current density and duration are. This is in good accordance with both our preliminary results, and with previous studies as increasing the amount of Zn²⁺ ions in electrolyte would enhance the carrier concentration [46]. This means that the ionic conductivity would increase up to a point, which was found between 50-60 g/L in our preliminary tests.

Although Table 4 suggests that none of the factors have a significant effect on the coating roughness, ZnCl₂ concentration is still the most important factor influencing it, as can be seen in Figure 4. However, unlike current efficiency, roughness tends to drop with the amount of Zn²⁺ ions in the electrolyte. For instance, Figure 4(e) shows the combined effect of current density and concentration at a constant duration of 3.5 min, and suggests that the roughness decreases with increasing both ZnCl₂ concentration and current density. Besides, Figure 4(f) shows that higher ZnCl₂ concentration could provide more smooth surfaces for longer testing durations, while roughness tends to be not affected by the concentration when the experiment duration is only 2 min at a constant current density of 4.5 A/dm².

Similar to the roughness, both Table 4 and Figure 4 (g and i) show that duration has almost no effect on the brightness of the coatings. When the mutual interaction between current density and concentration is examined together in Figure 4(h) at a constant duration of 3.5 min, it is found that the optimum value of current density to maximize the brightness seems to be about ~5 A/dm². Importantly, the dependence of brightness on the electrodeposition time is opposite at low and high ZnCl₂ concentrations, showing the importance of this mutual factor interaction. While, brightness decreases with electrodeposition time at low ZnCl₂ concentrations, it increases with electrodeposition time at higher ZnCl₂ concentrations as can be seen in Figure 4 (i). Also, it is interesting to note that both high and low concentrations of ZnCl₂ in electrolyte provide better brightness, while brightness reaches its minimum at about 30 g/L ZnCl₂ concentration depending on the electrodeposition time.

Overall, it could easily be seen from Table 2 and Figure 4 that optimized ZnCl₂ concentration is clearly 50 g/L. On the other hand, determination of optimum current density and electrodeposition time are rather complex due to the interaction effects of these factors. To simplify optimization, the coating thickness was introduced as a limiting variable. Since most relevant industrial applications necessitate a Zn film of about 6 μm, maximum allowable thickness value was set to 6 μm. Upon completion of the similar 18 CCD tests, the regression model for the coating thickness was also developed. This could be used in industrial applications as well for arranging input conditions to get a Zn coating of a desired thickness. Corresponding equation is given below, where (A), (B) and (C) represents the current density (A/dm²), electrodeposition time, and ZnCl₂ concentration, respectively:

$$\text{Thickness } (\mu\text{m}) = -0.35167 + 1.13833 A + 0.39167 B - 0.048333 C + 0.033333 AB + 0.0075 AC + 0.00416667 BC$$

Then, the optimization results of Design-Expert (trial version) is refined by taking the optimum ZnCl₂ concentration as 50 g/L, ignoring the roughness as none of the individual factors are statistically significant for it (see Table 3 and 4), and also setting a maximum film thickness of 6 μm. The corresponding data points are listed in Table 5. Finally, the optimum levels of current density and electrodeposition time are determined as 3.7 A/dm² and 4.4 min, respectively.

Table 5. List of electrodeposition parameters for maximizing the current efficiency and coating brightness up to a film thickness of 6 μm

No	Current density (A/dm ²)	Duration (min)	ZnCl ₂ concentration (g/L)	Current efficiency (%)	Brightness (L)	Thickness (μm)
1	3.59	4.63	50	97.95	81.86	6
2	3.6	4.62	50	97.98	81.86	6
3	3.55	4.73	50	97.79	81.88	6
4	3.47	4.92	50	97.44	81.93	6
5	3.59	4.59	50	98.02	81.83	5.98
6	3.66	4.45	50	98.27	81.80	5.98
7	3.86	4.02	50	98.99	81.66	6
8	3.61	4.46	50	98.21	81.77	5.91
9	3.9	3.92	50	99.15	81.63	6

3.3. Characterization of the Zn film that deposited at optimum conditions

A fresh Zn-A bath was prepared with the exception of ZnCl₂ concentration, which was set to 50 g/L instead of 40 g/L, to perform the electrodeposition at optimized conditions. Accordingly, the current density was set at 3.7 A/dm² and the corresponding voltage was applied for 4.4 minutes. The quality of as-prepared Zn films on 1010 steel cathodes were characterized in terms of brightness, color, thickness, roughness, adhesion and bending performances, as well as SEM and EDX analyses.

First, current efficiency was calculated as 98.7% by dividing the measured weight of the deposited Zn to its theoretical weight as explained in the experimental section. The average surface roughness was then measured by TMR200 roughness gauge as 0.75 μm . The results showed that a smooth Zn film was prepared with high current efficiency when the deposition was conducted at optimum conditions. Besides, both of these results were in good accordance with the model predictions of Design-Expert (trial version).



Figure 5. Macroscopic images (a and c) and optical microscope image (b) of the Zn film before (a and b) and after (c) a bending test

Color measurement was carried out by Konica Minolta CM-700d Spectrophotometer according to CIE L^*a^*b colour space as explained in the experimental section. The lightness value, L^* , was used to represent brightness as it indicates darkest black at $L^*=0$ and brightest white at $L^*=100$. Following the measurements under C illuminant at a 2 degree standard observer, the color values were determined as $L^*:83.69$, $a^*:-2.58$, $b^*:2.73$ and $YI:3.93$. Therefore, the surface was very bright as can also be seen from the macroscopic and optical microscope images at Figure 5(a and b). Besides, the measured brightness of Zn surface that deposited at optimum conditions was in good accordance with the model prediction of about 82.

Figure 6(a and c) shows the SEM images and EDX element mapping of the cross-section samples, respectively. As can be seen from Figure 6(a and c), a continuous Zn film was deposited on 1010 steel substrates. The SEM images suggested that the Zn coating exhibits a good adhesion with the steel. Besides, the thickness of the film was uniform and measured about $6.1 \mu\text{m}$ at Figure 6(a). In addition to this, the thickness was also measured by Mitutoyo micrometer and again, found about $6.1 \mu\text{m}$. Overall, the thickness results both obtained by SEM images and Mitutoyo micrometer are in good accordance with the model estimations ($\sim 6 \mu\text{m}$) of Design-Expert (trial version).

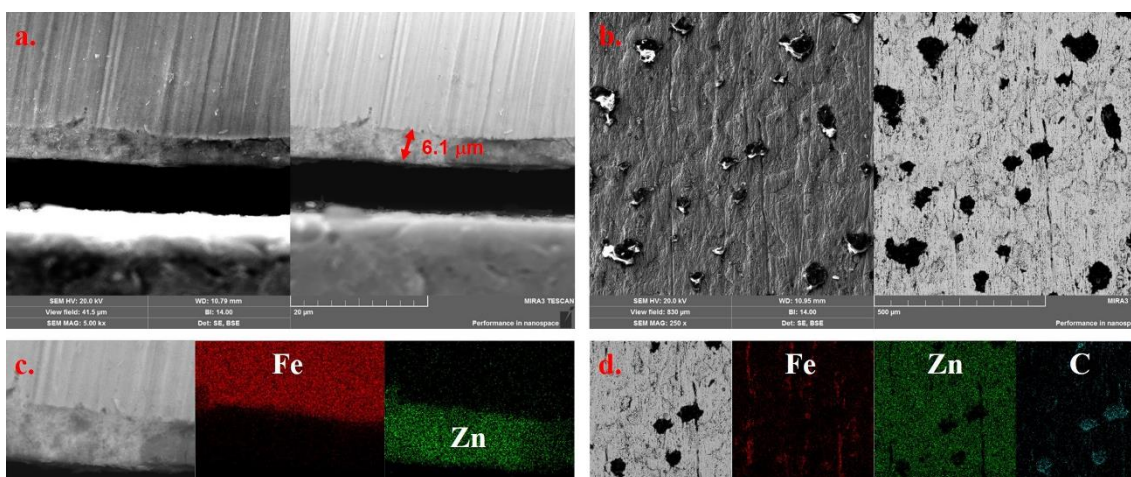


Figure 6. Cross-section SEM image (a), SEM image (b), cross-section EDX mapping (c) and EDX mapping (d) of the Zn film prior (a and c) and following to (b and d) adhesion test

Following this, an adhesion test was performed using PosiTest AT-M as explained in the experimental section. The pull-off strength was measured as 29.4 MPa. Figure 6(b and d) shows the SEM images and EDX analysis results of the coating following the adhesion test. The results suggest that most of the Zn film remained intact at the surface of steel substrate with only a few damaged regions coming from the epoxy based adhesive that applied to the surface prior to the pull-off test. This suggests that the adhesive connection between the Zn film and steel substrate was stronger than that of epoxy based resin and the Zn coating. Accordingly, the pull-off strength of Zn film on steel substrate should be higher than 29.4 MPa. In fact, this is in good accordance with previous reports as a much higher adhesion strength was recorded for physical vapor deposited Zn films on steel substrates, as well as estimations through theoretical work of adhesion calculations [48, 49].

A bending test was conducted as well to further comment on the quality of Zn coating. In this test, the samples were bent 90° using a simple system. Blistering was not observed on the coating as can be seen from the macroscopic image of the bended sample at Figure 5(c).

4. CONCLUSION

Zn films were prepared on 1010 steel substrates by electrodeposition. The conditions governing the quality of the deposited film such as current density, electrodeposition time and ZnCl₂ concentration were optimized to provide high current efficiency, together with a smooth and bright surface. Preliminary studies were conducted to determine the initial levels of designated factors to run the optimization procedure. Then, the optimization was conducted using CCD by Design-Expert (trial version). Accordingly, regression models of the response variables were developed, and they could be used in industrial applications to provide electrogalvanizing conditions for the preparation of desirable Zn coatings. Following the optimization, analysis of variance (ANOVA) was also performed to compare the experimental and model results. Overall, the experimental results were in good accordance with the model predictions. The optimum values of current density, electrodeposition time and ZnCl₂ concentration were found as 3.7 A/dm², 4.4 minutes, and 50 g/L respectively, upon setting a maximum allowable thickness value of 6 μm. Finally, a fresh bath was prepared to conduct the electrodeposition at this optimum conditions. Characterization of the deposited film at optimum conditions revealed that a bright ($L^*=83.69$) and smooth ($R_a=0.75$ μm) coating with a thickness of about 6.1 μm could be achieved at a high current efficiency of 98.7%. Besides, the Zn film showed an excellent adhesion with the steel substrate, having a pull-off strength of higher than 29.4 MPa and without any blistering even after 90° bending.

ACKNOWLEDGEMENTS

The authors would like to acknowledge the financial support from the Cumhuriyet University, Scientific Research Projects Commission (CUBAP).

References

1. A. Zaabar, E. Rocca, D. Veys-Renaux, R. Aitout, H. Hammache, L. Makhloufi and K. Belhamel, *Hydrometallurgy*, 191 (2020) 105186.

2. H. B. Muralidhara and Y. Arthoba Naik, *Surface and Coatings Technology*, 202 (2008) 3403-3412.
3. R. E. Elewa, S. A. Afolalu and O. S. I. Fayomi, *Journal of Physics: Conference Series*, 1378 (2019).
4. P. P. Chung, J. Wang and Y. Durandet, *Friction*, 7 (2019) 389-416.
5. H. Katayama and S. Kuroda, *Corrosion Science*, 76 (2013) 35-41.
6. N. M. Chavan, B. Kiran, A. Jyothirmayi, P. S. Phani and G. Sundararajan, *Journal of Thermal Spray Technology*, 22 (2013) 463-470.
7. S. Matthews and B. James, *Journal of Thermal Spray Technology*, 19 (2010) 1277-1286.
8. P. Bicao, W. Jianhua, S. Xuping, L. Zhi and Y. Fucheng, *Surface and Coatings Technology*, 202 (2008) 1785-1788.
9. J. D. Culcasi, P. R. Sere', C. I. Elsner and A. R. Di Sarli, *Surface and Coatings Technology*, 122 (1999) 21-23.
10. D. Sansom, F. Alonso, J. J. Ugarte, F. Zapirain and J. I. Ofiate, *Surface and Coatings Technology*, 84 (1996) 480-484.
11. C. A. Loto, *Asian Journal of Applied Sciences*, 5 (2012) 314-326.
12. C. A. Loto, R. T. Loto and A. P. Popoola, *Journal of Bio- and Tribo-Corrosion*, 6 (2019).
13. I. W. Wark, *Journal of Applied Electrochemistry*, 9 (1979) 721-730.
14. C. Oulmas, S. Mameri, D. Boughrara, A. Kadri, J. Delhalle, Z. Mekhalif and B. Benfedda, *Heliyon*, 5 (2019) e02058.
15. N. Sorour, W. Zhang, E. Ghali and G. Houlachi, *Hydrometallurgy*, 171 (2017) 320-332.
16. M. Mouanga, L. Ricq, L. Ismaili, B. Refouvelet and P. Berçot, *Surface and Coatings Technology*, 201 (2007) 7143-7148.
17. P. Diaz-Arista, Y. Meas, R. Ortega and G. Trejo, *Journal of Applied Electrochemistry*, 35 (2005) 217-227.
18. K. M. S. Youssef, C. C. Koch and P. S. Fedkiw, *Corrosion Science*, 46 (2004) 51-64.
19. Joo-Yul Lee, Jae-Woo Kim, Min-Kyu Lee, Hyun-Joon Shin, Hyun-Tae Kim and S.-M. Park, *Journal of the Electrochemical Society*, 151 (2004) C25-C31.
20. G. Trejo, H. Ruiz, R. Ortega Borges and Y. Meas, *Journal of Applied Electrochemistry*, 31 (2001) 685-692.
21. C. A. Loto and R. T. Loto, *Int. J. Electrochem. Sci.*, 8 (2013) 12434-12450.
22. C. A. Loto and R. T. Loto, *Polish Journal of Chemical Technology*, 15 (2013) 38-45.
23. M. Rahsepar and M. E. Bahrololoom, *Surface and Coatings Technology*, 204 (2009) 580-585.
24. M. H. Gharahcheshmeh and M. H. Sohi, *Materials Chemistry and Physics*, 117 (2009) 414-421.
25. C. Savall, C. Rebere, D. Sylla, M. Gadouleau, P. Refait and J. Creus, *Materials Science and Engineering: A*, 430 (2006) 165-171.
26. H. Park and J. A. Szpunar, *Corrosion Science*, 40 (1998) 525-545.
27. Z. Zhang and M. L. Free, *Jom*, 71 (2019) 1623-1633.
28. S. Anwar, F. Khan, Y. Zhang and S. Caines, *The Canadian Journal of Chemical Engineering*, 97 (2019) 2426-2439.
29. F. B. A. Ferreira, F. L. G. Silva, A. S. Luna, D. C. B. Lago and L. F. Senna, *Journal of Applied Electrochemistry*, 37 (2007) 473-481.
30. A. Y. Musa, Q. J. M. Slaiman, A. A. H. Kadhum and M. S. Takriff, *European Journal of Scientific Research*, 22 (2008) 517-524.
31. D. S. Baik and D. J. Fray, *Journal of Applied Electrochemistry*, 31 (2001) 1141-1147.
32. S. Ganesan, G. Prabhu and B. N. Popov, *Surface and Coatings Technology*, 238 (2014) 143-151.
33. H. Kazimierzak, P. Ozga, A. Jałowiec and R. Kowalik, *Surface and Coatings Technology*, 240 (2014) 311-319.

34. M. Bučko, J. Rogan, B. Jokić, M. Mitrić, U. Lačnjevac and J. B. Bajat, *Journal of Solid State Electrochemistry*, 17 (2013) 1409-1419.
35. L. Mirkova, G. Maurin, I. Krastev and C. Tsvetkova, *Journal of Applied Electrochemistry*, 31 (2001) 647-654.
36. R. Ichino, C. Cachet and R. Wiart, *Electrochimica Acta*, 41 (1996) 1031-1039.
37. C. Cachet and R. Wiart, *Journal of Applied Electrochemistry*, 20 (1990) 1009-1014.
38. M. C. Li, S. S. Xin and M. Y. Wu, *Journal of Solid State Electrochemistry*, 14 (2010) 2235-2240.
39. T. Casanova, F. Soto, M. Eyraud and J. Crousier, *Corrosion Science*, 39 (1997) 529-537.
40. T. Zakroczymski, V. Kleshnya and J. Flis, *Journal of Electrochemical Society*, 145 (1998).
41. M. H. Abd Elhamid, B. G. Ateya and H. W. Pickering, *Journal of Electrochemical Society*, 144 (1997) L58-L61.
42. M. A. V. Devanathan and Z. Stachurski, *Journal of the Electrochemical Society*, 111 (1964) 619-623.
43. H. B. Muralidhara, Y. Arthoba Naik and T. V. Venkatesha, *Bulletin of Materials Science*, 29 (2006) 497-503.
44. Yanjerappa Arthoba Naik, Thimmappa Venkatarangaiah Venkatesha and P. V. Nayak, *Turkish Journal of Chemistry*, 26 (2002) 725-733.
45. M. Sagiya, T. Urakawa, T. Adaniya, T. Hara and Y. Fukuda, *Plating and Surface Finishing*, 74 (1987) 77-82.
46. A. C. Scott, R. M. Pitblado and G. W. Barton, *Journal of Applied Electrochemistry*, 18 (1988) 120-127.
47. G. Trejo, O. R.B., M. Y.V., P. Ozil, E. Chainet and B. Nguyen, *Journal of Electrochemical Society*, 145 (1998) 4090-4097.
48. S. Sabooni, M. Ahmadi, E. Galinmoghaddam, R. J. Westerwaal, C. Boelsma, E. Zoestbergen, G. M. Song and Y. T. Pei, *Materials & Design*, 190 (2020).
49. S. Sabooni, E. Galinmoghaddam, M. Ahmadi, R. J. Westerwaal, J. van de Langkruis, E. Zoestbergen, J. T. M. De Hosson and Y. T. Pei, *Surface and Coatings Technology*, 359 (2019) 227-238.